Chemical Science

Accepted Manuscript

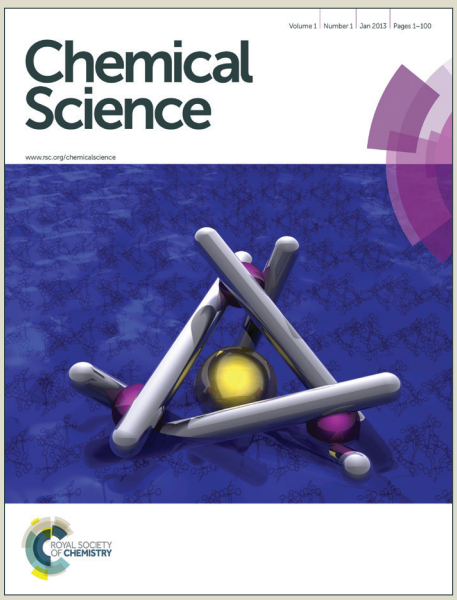

ROYAL SOCIETY OF CHEMISTRY

www.rsc.org/chemicalscience

Journal Name RSCPublishing

ARTICLE

Electrostatic Control of Regioselectivity via Ion Pairing in a Au(I)–Catalyzed Rearrangement†

Cite this: DOI: 10.1039/x0xx00000x

Vivian M. Lau [a], Craig F. Gorin [a] and Matthew W. Kanan [*a],

Received 00th January 2012,
Accepted 00th January 2012

DOI: 10.1039/x0xx00000x

www.rsc.org/

The rearrangement of 3-substituted aryl alkynyl sulfoxides catalyzed by cationic Au(I) complexes was studied with different counterions in solvents spanning a range of dielectric constants (ε). Pulsed-gradient diffusion NMR experiments demonstrated strong ion pairing in low-ε solvents. The regioselectivity of the reaction was insensitive to ε when ion pairing was weak but increased monotonically as ε was decreased in the regime of strong ion pairing. DFT calculations of putative product-determining transition states indicated that the product resulting from the more polar transition state is favored due to electrostatic stabilization in the presence of strong ion pairing.

Introduction

Ion pairing has been widely exploited to control the rate and selectivity of reactions that involve charged species.[1-5] In the strategies that have been developed to date, counterions have been used to promote phase transfer, create new steric and chemical environments, bind weakly to reactive centers, participate directly in chemical reactions, or a combination of the above. Because of its proximity to a reactive species in an ion pair, a counterion could in principle affect the selectivity of a reaction through electrostatic interactions that differentiate competing transition states. Although the major electrostatic interaction is the charge–charge attraction that holds an ion pair together, transition states that have significantly different *charge distributions* could be (de)stabilized to different extents by the local electric field generated by a counterion.[6-9] Here we show that ion pairing changes the regioselectivity of a Au(I)-catalyzed aryl alkynyl sulfoxide rearrangement by favoring the product resulting from a more polar transition state through electrostatic interactions.

Results and discussion

Previous studies have shown that Au(I) complexes catalyze a rearrangement of aryl alkynyl sulfoxides to dihydrobenzothiepinones, a transformation that replaces an aryl C–H bond with a C–C bond.[10-12] To study regioselectivity for this reaction, we prepared 3-Cl aryl alkynyl sulfoxide **1a**, for which C–H functionalization can occur at either the 2- or 6-position. We first assessed the effects of ligand structure on selectivity using a series of common phosphine (R_3P) and *N*-heterocyclic carbene (NHC) ligands (Table 1). **1a** was reacted with 2 mol% R_3PAuCl or NHCAuCl precatalyst and 2 mol%

Table 1. Ligand influence on regioselectivity.

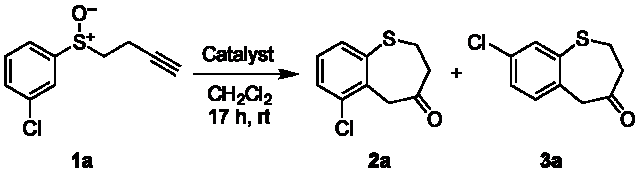

Entry	Catalyst (2 mol%)	**3a**:**2a**[a]	Yield (%)[b]
1	**IMes**AuCl / $NaBAr^F{}_4$	0.7 : 1	46
2	**IPr**AuCl / $NaBAr^F{}_4$	1.3 : 1	32
3	**SIPr**AuCl / $NaBAr^F{}_4$	1.9 : 1	78
4	**Ph_3P**AuCl / $NaBAr^F{}_4$	0.6 : 1	25
5	**(*o*-tol)$_3$P**AuCl / $NaBAr^F{}_4$	0.6 : 1	30
6	**SPhos**AuCl / $NaBAr^F{}_4$	0.6 : 1	32
7	**XPhos**AuCl / $NaBAr^F{}_4$	0.6 : 1	46

[a]Determined by NMR of crude reaction mixture. [b]Determined by NMR using an internal standard.

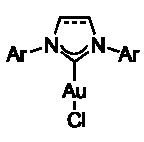

IMes: Ar = 2,4,6-$Me_3C_6H_2$
IPr: Ar = 2,6-$iPr_2C_6H_3$
SIPr: Ar = 2,6-$iPr_2C_6H_3$, saturated

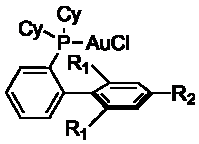

SPhos: R_1 = OMe, R_2 = H
XPhos: R_1 = R_2 = *i*Pr

$NaBAr^F_4$ (Ar^F = 3,5-$(CF_3)_2C_6H_3$) in CH_2Cl_2 at room temperature for 17 h. $NaBAr^F_4$ serves as a Cl^- abstractor to generate an active cationic $R_3PAu(I)$ or NHCAu(I) catalyst. These conditions gave clean conversion to the two expected regioisomeric products **2a** and **3a** in moderate to good yields and recovery of the starting material. For NHCAu(I) catalysts, increasing the steric demand of the NHC (IMes < IPr < SIPr)[13] increased the **3a**:**2a** ratio from 0.7:1.0 to 1.9:1.0, favoring functionalization at the more accessible C–H bond (Table 1, entries 1–3). For the $R_3PAu(I)$ catalysts with R_3P = Ph_3P, (*o*-tol)$_3$P, SPhos, or XPhos, the selectivity was completely insensitive to ligand structure. The ratio of **3a**:**2a** was 0.6:1.0 with all of these catalysts despite their substantially different steric and electronic properties (Table 1, entries 4–7).[13] Overall, the ligand screen highlights the difficulty of controlling regioselectivity for this aryl C–H functionalization by changing the ligand structure.

To test whether ion pairing could affect selectivity, we performed the reaction with different counterions in solvents that span a range of dielectric constants (ε). Nitrile complexes [NHCAu(NCR)]X and [R_3PAu(NCR)]X (X = anion) were used as pre-catalysts in these experiments to obviate Cl^- abstraction. Spontaneous dissociation of NCR generates the catalytically active cationic Au(I) complex. The reactions were performed with 2.5 mM **1a** and 2 mol% catalyst loading at room temperature. The reactions were stopped after 4 h to determine the product ratio using ^{1}H NMR. Unoptimized yields varied from 22% to 88% depending on the ligand (Table S2). Recovered substrate **1a** accounted for essentially all of the remaining material.

The dielectric constant of the solvent affected the regioselectivity obtained with each of the Au(I)-catalysts in a counterion-dependent manner. The results for NHCAu(I) complexes are shown in Figure 1a. With [IPrAu(NCPh)]BAr^F_4, the solvent had little effect on selectivity. The **3a**:**2a** ratio ranged from 0.8:1.0 to 1.2:1.0 across seven solvents with ε ranging from 2.4 (toluene) to 20.7 (acetone). With [IPrAu(NCMe)]SbF_6, however, a significant solvent dependence was observed. For solvents with ε ≥ 8.9 (CH_2Cl_2, $(CH_2Cl)_2$, acetone), the **3a**:**2a** ratio was similar to the ratio with the $BAr^F_4{}^-$ complex. For solvents with ε ≤ 6.0, the ratio increased monotonically as ε decreased, reaching 2.7:1.0 in toluene. The same trend was observed with [IPrAu(NCMe)]BF_4, but the increase in the ratio for ε ≤ 6.0 was attenuated. Thus, the counterion determined the dependence of the selectivity on ε, with the magnitude given by the order SbF_6^- > BF_4^- > $BAr^F_4{}^-$ ≈ 0. The same solvent and counterion dependencies were observed with the IMes and SIPr complexes (Figure 1a and Table S2). These effects *added* to the effects of the steric properties of the ligand such that the largest **3a**:**2a** ratio, 4.5:1.0, was obtained with [SIPrAu(NCMe)]SbF_6 in toluene.

Larger counterion-dependent responses to ε were obtained with phosphine complexes. Since $BAr^F_4{}^-$ complexes proved to be unstable in solution, we compared complexes with SbF_6^-, PF_6^-, and BF_4^- counterions. The same trends were observed in all cases: the **3a**:**2a** ratio showed essentially no dependence on ε for solvents with an ε > 8, but increased monotonically as ε

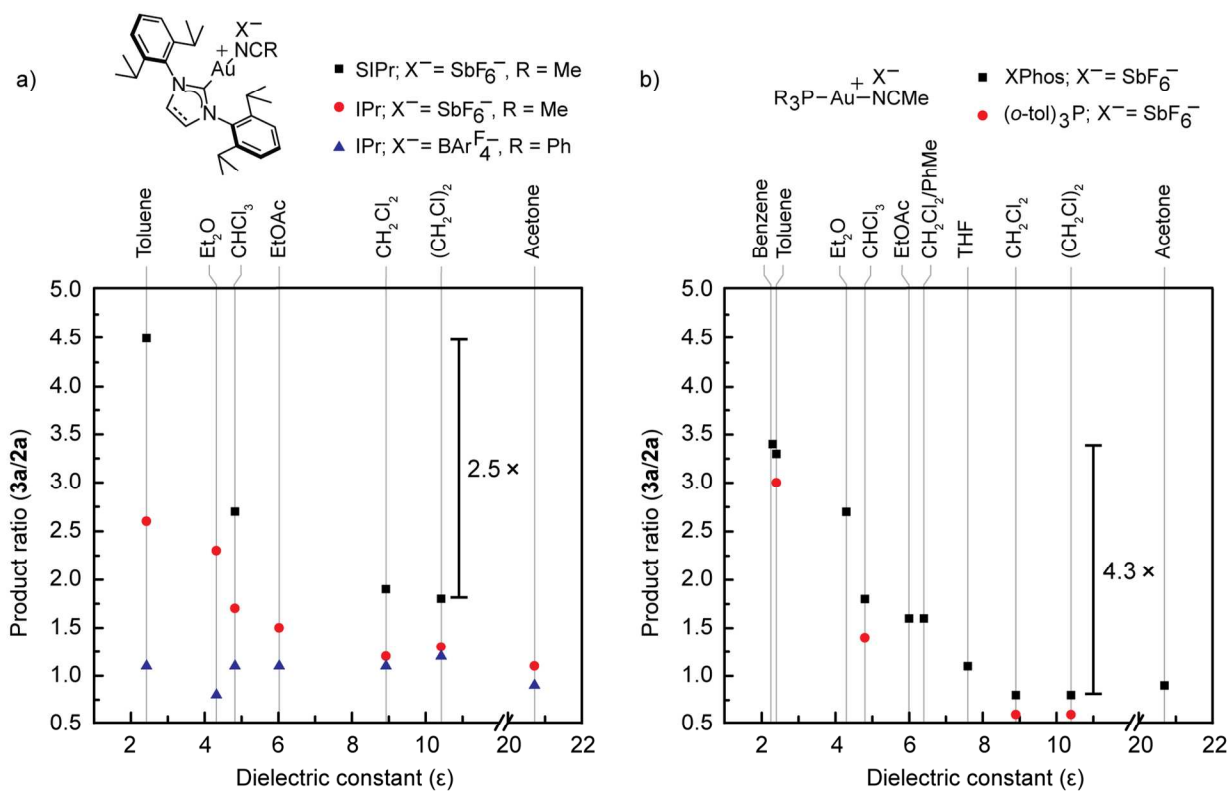

Figure 1. Effect of solvent dielectric on product ratio for substrate **1a**, catalyzed by [NHCAu(NCR)]X (a) and [R_3PAu(NCMe)]X (b). Magnitude of the dielectric response is dependent on the ligand and identity of counterion X^-.

was decreased below 8 (Figure 1b). The changes were significantly larger with SbF_6^- than with PF_6^- or BF_4^- and they varied with the phosphine structure in the order XPhos ≈ (*o*-tol)$_3$P > Ph$_3$P (Table S2). With XPhos and (o-tol)$_3$P ligands and SbF_6^- counterion, the **3a**:**2a** ratio increased by a factor of 4.3–5.0 in going from ε = 8.9 (CH_2Cl_2) to ε = 2.4 (toluene). Only the solvent's ε impacted selectivity and not its molecular properties (dipole moment, coordinating ability, etc.) The product ratios obtained in solvent mixtures matched the expected value for their calculated ε.

The dependence of the product ratio on ε and the choice of counterion suggests that the selectivity-determining step proceeds from an ion-paired intermediate in low-ε solvents. Previous diffusion NMR studies of many organometallic complexes have shown that ion pairing is strongly favored in $CDCl_3$ and less polar solvents.[14, 15] Weaker, but still substantial, ion pairing has been observed for cationic R$_3$PAu(I) and NHCAu(I) complexes paired with BF_4^- in CD_2Cl_2.[16-18] To assess the extent of ion pairing for the catalysts used here, we performed pulsed gradient spin echo (PGSE) diffusion ^{1}H NMR measurements using 5 mM solutions of [IPrAu(NCPh)]BAr$^F_4$, and [IPrAu(NCMe)]SbF_6 in CD_2Cl_2 and $CDCl_3$ at 25 °C. The diffusion coefficients (*D*) of the ions were obtained from Stejskal-Tanner plots (Figure S1). To compare between CD_2Cl_2 and $CDCl_3$, the hydrodynamic radii (r_H) of the ions were calculated using the Stokes–Einstein equation (see Supporting Information). An increase in the r_H value from one solvent to another indicates an increase in the extent of ion pairing.[14]

^{1}H PGSE NMR measurements of [IPrAu(NCPh)]BAr$^F_4$ yielded an r_H value for the cation that increased from 6.6 Å in CD_2Cl_2 to 7.2 Å in $CDCl_3$, and an r_H for the anion that increased from 6.6 Å to 7.3 Å (Table 2). Since the molecular radius of [IPrAu(NCPh)]BAr$^F_4$ estimated from the crystallographic cell volume is 7.3 Å,[19] the r_H values in $CDCl_3$ are consistent with complete ion pairing in this solvent. This result also suggests that ion pairing is likely strongly favored in $CDCl_3$ for all complexes studied here because BAr$^F_4^-$ is larger and much more lipophilic than the other counterions. The smaller r_H values for $BArF_4^-$ and [IPrAu(NCPh)]$^+$ in CD_2Cl_2 indicate much weaker ion pairing in this solvent. ^{1}H PGSE measurements of additional complexes indicated that the hydrodynamic radii for unpaired [IPrAu(NCPh)]$^+$ and BAr$^F_4^-$ were ~6.3 Å and ~6.4 Å, respectively (Table S1). For [IPrAu(NCPh)]SbF_6, only the cation r_H values could be obtained because the quadrupole moment of Sb renders the SbF_6^- species ^{19}F NMR-silent. The cation r_H for this complex increased from 5.8 Å in CD_2Cl_2 to 6.3 Å in $CDCl_3$, again indicating much stronger ion pairing in $CDCl_3$.

Table 2. Solvent dependence of the diffusion coefficient *D* (10^{-10} m^2/s) and hydrodynamic radius r_H (Å) of representative Au(I) complexes.

Complex	Solvent		*D*	r_H
[IPrAu(NCPh)]BAr$^F_4$	$CDCl_3$	Cation	6.0	7.2
		Anion	5.9	7.3
	CD_2Cl_2	Cation	8.7	6.6
		Anion	8.7	6.6
[IPrAu(NCMe)]SbF_6	$CDCl_3$	Cation	7.0	6.3
	CD_2Cl_2	Cation	10.3	5.8

The diffusion NMR results, combined with extensive data from other organometallic complexes,[14, 15, 17, 18] indicates that the equilibria strongly favor the ion paired forms for the NHCAu(I) and R$_3$PAu(I) complexes in $CDCl_3$ and all less polar solvents. The monotonic increase of the **3a**:**2a** ratio as ε is decreased below 8 for all complexes therefore is not likely the result of a significant increase in the extent of ion pairing but instead reflects an increased strength of the *effect* of the counterion on the product-determining transition states (see below).

To gain further insight into the origin of the ion pairing effect, we explored its dependence on the aryl substituent. Additional 3-substituted aryl alkynyl sulfoxides **1b** – **1f** were reacted with [(*o*-tol)$_3$PAu(NCMe)]SbF_6 to yield regioisomeric products **2b** – **2f** and **3b** – **3f**. Figure 2 shows the product ratios, **3x**:**2x**, in CH_2Cl_2, $CHCl_3$, and toluene. The magnitude of the change in product ratio from high ε (CH_2Cl_2) to low ε (toluene) exhibited a strong dependence on the substituent. Me-substituted **1b** showed essentially no response to the change in ε. For the rest of the substrates, the **3x**:**2x** ratio increased from high e to low e, with the magnitude of the change given by the order OMe<Br<F<Cl<CF_3 (Table 3). For CF_3-substituted **1f**, the ratio increased by a factor of 6.3. In all of these cases, a smaller increase was obtained in $CHCl_3$ compared to toluene, consistent with the trend evident in Figure 1.

The absence of a correlation between the size of the substituent and the magnitude of the selectivity change from high-ε to low-ε solvent indicates that ion pairing does not principally affect selectivity via steric interaction. The results in

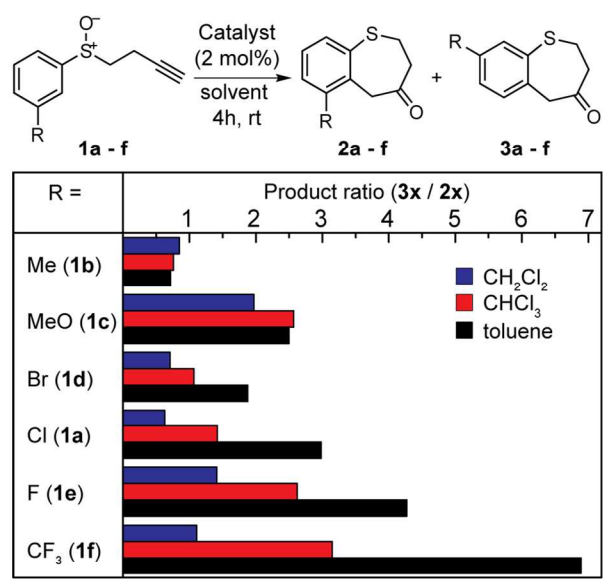

Figure 2. Substrate-dependent change in regioselectivity in CH_2Cl_2, $CHCl_3$ and toluene. Catalyst = [(*o*-tol)$_3$PAu(NCMe)]SbF_6.

Figures 1 and 2 instead implicate an electrostatic effect of the counterion on the energy barriers leading to the two products.

Table 3. Calculated dipole moments of isomeric transition states leading to products **2x and 3x.**

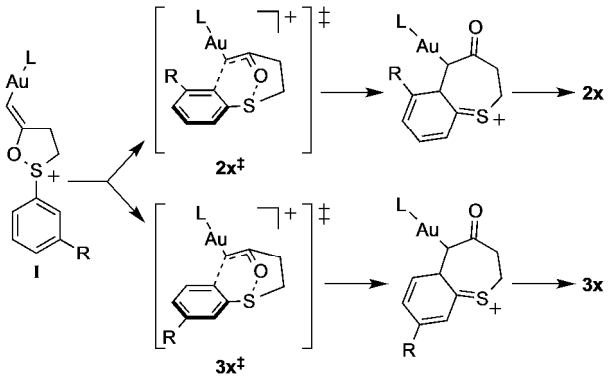

R =	Transition state dipole moment ρ(**2x**‡) (D)	ρ(**3x**‡) (D)	Δ|ρ| (D)	$\frac{P_{toluene}}{P_{CH_2Cl_2}}$ [a]
Me (**1b**)	4.1	4.0	–0.1	0.9
MeO (**1c**)	4.1	4.8	0.7	1.3
F (**1e**)	2.9	5.4	2.5	3.1
Cl (**1a**)	2.6	5.9	3.3	5.0
Br (**1d**)	2.5	7.5	5.0	2.7
CF_3 (**1f**)	2.4	9.0	6.6	6.3

[a] $P_{toluene}$ and P_{CH2Cl2} are the product ratios (**3x**/**2x**) in toluene and CH_2Cl_2.

To probe electrostatic differences between the reactions with

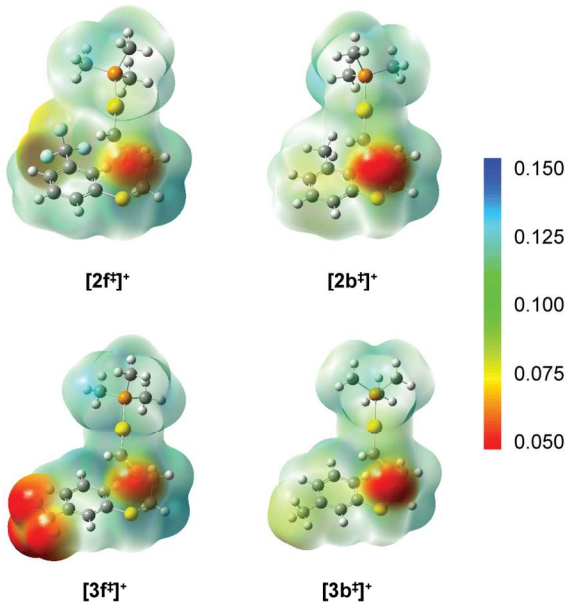

Figure 3. Charge density maps of the product-determining transition states for substrates with CH_3 ([**2b**‡]$^+$, [**3b**‡]$^+$) and CF_3 ([**2f**‡]$^+$, [**3f**‡]$^+$) substituents.

different substrates, DFT calculations were performed for putative product-determining transition states for each substrate. Recent experimental and computational studies provide strong evidence that C–C bond formation occurs through an irreversible [3,3]-sigmatropic rearrangement of a cationic vinyl Au intermediate **I** (Table 3).[12, 20, 21] We calculated the [3,3] transition state leading to each regioisomer for the substrates in Figure 2 with a model Me_3P-Au(I) catalyst. We then calculated a dipole moment (ρ) for each transition state using the center of nuclear charge as the origin. Figure 3 shows the charge density maps for the regioisomeric transition states for substrates **1b** and **1f**. The difference in the magnitude of the dipole moments (Δ|ρ|) indicates the extent to which the transition states differ in their charge distributions. The calculations revealed a strong correlation between Δ|ρ| and the magnitude of the change in the product ratio upon switching from CH_2Cl_2 to toluene: Δ|ρ| ≈ 0 with CH_3-substituted sulfoxide and increased in the order OMe < F < Cl < Br < CF_3 (Table 3).

Ion pairing favored the isomer (**3a**, **3c**–**3f**) that is formed from the more polar product-determining transition state. This result indicates that the paired anion electrostatically stabilizes the transition state leading to the major product to a greater extent than it stabilizes the competing transition state. The strength of the electrostatic interactions that energetically differentiate the two transition states depends on the ε of the medium surrounding the ion pair, which explains why selectivity continues to rise as ε is decreased below 5 even though it is unlikely that the extent of ion pairing changes appreciably in this regime. The ion pairing effect is in contrast to the absence of a response to solvent polarity when ε ≥ 8. Increasing ε does not significantly favor the pathway proceeding through the more polar transition state whereas ion pairing in a low-ε medium does.

In addition to the substrate, the strength of the ion pairing effect depends on the structure of both the counterion and the ligand. This dependence most likely reflects changes to the placement(s) of the counterion in the ion pair. Maximum electrostatic differentiation of transition states requires placing the counterion as close as possible to the complex and in a position where it can afford the greatest stabilization to the more polar transition state. No effect is seen when pairing with $BAr^F{}_4^-$ because its large radius places negative charge too far away. The difference between SbF_6^- and PF_6^- or BF_4^- suggests that SbF_6^- is better positioned in the ion pair. The relatively small ion pairing effect for Br-substituted **1d** given the large Δ|ρ| for this substrate may also reflect poor counterion placement. Additional nuclear Overhauser effect NMR studies[17, 22, 23] and molecular dynamics simulations will be necessary to shed light on these important structural details. Tuning the ligand and counterion structure to adjust ion placement may substantially increase the selectivity afforded by this approach.

Conclusions

In summary, we have demonstrated that ion pairing can control selectivity by preferentially stabilizing more polar

transition states. This strategy may be applicable to diverse synthetic challenges because many reactions involve competing pathways with significantly different charge distributions.

Acknowledgements

We thank Stanford University, the Air Force Office of Scientific Research (FA9550-11-1-0293), the NSERC (Canada) PGS-D Fellowship (V.M.L.), and the Gerald J. Lieberman Fellowship (C.F.G.) We also thank Dr. S. Lynch for assistance with diffusion NMR and the Stack lab for use of the Redox Cluster for computations.

Notes and references

[a] Department of Chemistry, Stanford University, 337 Campus Drive, Stanford, California 94305, United States. Email: mkanan@stanford.edu

† Electronic Supplementary Information (ESI) available: Experimental details, supplementary tables and figures, characterization data. CCDC 1013545. See DOI: 10.1039/b000000x/

1. C. M. Starks, C. L. Liotta and M. Halpern, *Phase-Transfer Catalysis*, Chapman & Hall, New York, NY, 1994.
2. M. Delferro and T. J. Marks, *Chem Rev*, 2011, 111, 2450–2485.
3. S. E. Denmark, N. D. Gould and L. M. Wolf, *Journal of Organic Chemistry*, 2011, 76, 4337-4357.
4. K. Brak and E. N. Jacobsen, *Angew Chem Int Edit*, 2013, 52, 534-561.
5. M. Mahlau and B. List, *Angew Chem Int Edit*, 2013, 52, 518-533.
6. A. Warshel, P. K. Sharma, M. Kato, Y. Xiang, H. B. Liu and M. H. M. Olsson, *Chem Rev*, 2006, 106, 3210-3235.
7. S. G. Boxer, *J Phys Chem B*, 2009, 113, 2972-2983.
8. C. F. Gorin, E. S. Beh and M. W. Kanan, *J Am Chem Soc*, 2012, 134, 186-189.
9. C. F. Gorin, E. S. Beh, Q. M. Bui, G. R. Dick and M. W. Kanan, *J Am Chem Soc*, 2013, 135, 11257-11265.
10. N. D. Shapiro and F. D. Toste, *J Am Chem Soc*, 2007, 129, 4160-+.
11. G. T. Li and L. M. Zhang, *Angew Chem Int Edit*, 2007, 46, 5156-5159.
12. B. Lu, Y. X. Li, Y. L. Wang, D. H. Aue, Y. D. Luo and L. M. Zhang, *J Am Chem Soc*, 2013, 135, 8512-8524.
13. H. Clavier and S. P. Nolan, *Chem Commun*, 2010, 46, 841-861.
14. A. Macchioni, G. Ciancaleoni, C. Zuccaccia and D. Zuccaccia, *Chem Soc Rev*, 2008, 37, 479-489.
15. P. S. Pregosin, P. G. A. Kumar and I. Fernandez, *Chem Rev*, 2005, 105, 2977-2998.
16. P. S. Pregosin, *Prog Nucl Mag Res Sp*, 2006, 49, 261-288.
17. D. Zuccaccia, L. Belpassi, F. Tarantelli and A. Macchioni, *J Am Chem Soc*, 2009, 131, 3170-+.
18. G. Ciancaleoni, L. Belpassi, F. Tarantelli, D. Zuccaccia and A. Macchioni, *Dalton T*, 2013, 42, 4122-4131.
19. N. Huguet, D. Leboeuf and A. M. Echavarren, *Chem-Eur J*, 2013, 19, 6581-6585.
20. A. B. Cuenca, S. Montserrat, K. M. Hossain, G. Mancha, A. Lledos, M. Medio-Simon, G. Ujaque and G. Asensio, *Org Lett*, 2009, 11, 4906–4909.
21. C. Obradors and A. M. Echavarren, *Chem Commun*, 2014, 50, 16-28.
22. D. Zuccaccia, L. Belpassi, A. Macchioni and F. Tarantelli, *Eur J Inorg Chem*, 2013, 2013, 4121-4135.
23. D. Zuccaccia, L. Belpassi, L. Rocchigiani, F. Tarantelli and A. Macchioni, *Inorg Chem*, 2010, 49, 3080-3082.